Electronic Supplementary Information (ESI)

Comprehensive control of voltage loss enables 11.7% efficient solid-state dye-sensitized solar cells†

Weiwei Zhang,[ab] Yongzhen Wu,*[a] Hee Won Bahng,[c] Yiming Cao,[b] Chenyi Yi,[b] Yasemin Saygili,[d] Jingshan Luo,[b] Yuhang Liu,[b] Ladislav Kavan,[ae] Jacques-E. Moser,[c] Anders Hagfeldt,[d] He Tian,[a] Shaik Mohammed Zakeeruddin,*[b] Wei-Hong Zhu*[a] and Michael Grätzel*[b]

[a]*Key Laboratory for Advanced Materials and Institute of Fine Chemicals, Shanghai Key Laboratory of Functional Materials Chemistry, School of Chemistry and Molecular Engineering, East China University of Science and Technology, Shanghai 200237, China. E-mail: wu.yongzhen@ecust.edu.cn, whzhu@ecust.edu.cn*

[b]*Laboratory of Photonics and Interfaces, Institute of Chemical Sciences and Engineering, École Polytechnique Fédérale de Lausanne (EPFL), 1015 Lausanne, Switzerland. E-mail: shaik.zakeer@epfl.ch, michael.graetzel@epfl.ch*

[c]*Photochemical Dynamics Group, Institute of Chemical Sciences and Engineering, École Polytechnique Fédérale de Lausanne (EPFL), 1015 Lausanne, Switzerland.*

[d]*Laboratory of Photomolecular Science, Institute of Chemical Sciences and Engineering, École Polytechnique Fédérale de Lausanne (EPFL), 1015 Lausanne, Switzerland.*

[e]*J. Heyrovsky Institute of Physical Chemistry, 1823 Prague, Czech Republic.*

Contents

1. **Photophysical data for dyes Y123, WS-70 and WS-72.**
2. **Cyclic voltammograms of dyes Y123, WS-70 and WS-72 adsorbed on TiO_2 films**
3. **Photovoltaic performance of DSSCs fabricated with dyes Y123, WS-70 and WS-72 using different electrolytes**
4. **Photophysical and kinetic analysis**
5. **Evolution of photovoltaic performances**
6. **Element mapping of the dispersion of Cu and Ti elementary in the mesoporous TiO_2 film**
7. **Comparison of electron injection efficiency**
8. **Synthesis and characterizations**

1. Photophysical data for dyes Y123, WS-70 and WS-72

Table S1 Photophysical data for dyes **Y123**, **WS-70** and **WS-72**.

Dye	λ_{max} [nm]^a	ε [M^{-1} cm^{-1}]^a	λ_{max} on TiO_2 [nm]^b
Y123	541	52406	486
WS-70	542	62251	514
WS-72	545	58765	514

[a] Absorption maximum and molar extinction coefficients measured in dichloromethane solution.

[b] Absorption maximum obtained from dye-adsorbed onto 2 μm thick transparent TiO_2 films.

2. Cyclic voltammograms of dyes Y123, WS-70 and WS-72 adsorbed on TiO_2 films

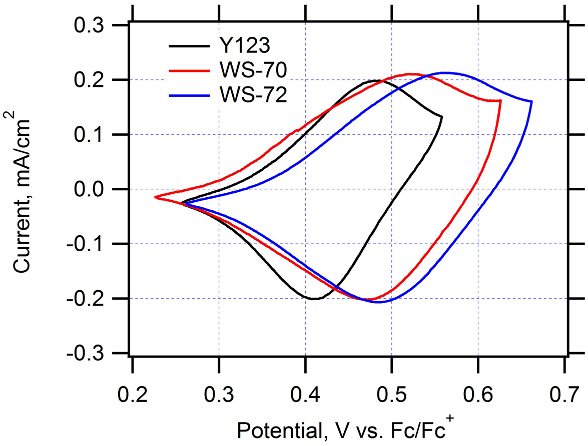

Fig. S1 Cyclic voltammograms of dyes **Y123**, **WS-70** and **WS-72** adsorbed on TiO_2 films.

Cyclic voltammetry of dyes was investigated using an Autolab potentiostat (Metrohm). This procedure was mandatory to obtain accurate values of redox potentials under the working condition of DSSCs. Dyes were adsorbed on the FTO-supported TiO_2 films. Electrolyte solution was 0.1 M LiTFSI in acetonitrile. Three-electrode cell was assembled with an Ag/AgCl (sat. LiCl in ethanol) reference electrode and a Pt-wire auxiliary electrode. The reference electrode was interfaced to a fritted bridge containing the same supporting electrolyte solution as the tested system. For the working electrode fabrication, the FTO-supported, dye-sensitized TiO_2 film was used. This electrode is essentially identical to that used in actual DSSCs, except for the $TiCl_4$ treatment that was omitted in this case. Ferrocene served as the internal standard for calibration of the Ag/AgCl electrode and accurate measurement of redox potentials. To get the potentials in the NHE scale, a correction factor of 0.63 V was added.

3. Photovoltaic performances of DSSCs fabricated with dyes Y123, WS-70 and WS-72 with different redox electrolytes

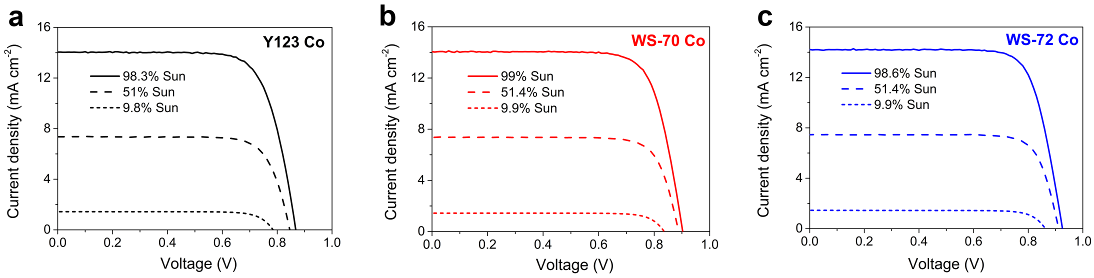

Fig. S2 *J*-*V* curves of the DSSCs fabricated with dye **Y123** (**a**), **WS-70** (**b**) and **WS-72** (**c**) employing $[Co(bpy)_3]^{3+/2+}$ based electrolyte measured under different light intensities (solid, 1 Sun; dashed, 0.5 Sun; dot, 0.1 Sun).

Table S2 Photovoltaic performances of DSSCs fabricated with dyes **Y123**, **WS-70** and **WS-72** with $[Co(bpy)_3]^{3+/2+}$ based electrolyte measured under varied light intensities.

Dye	P_{in} (mW/cm^2)	J_{SC} (Cal) (mA cm^{-2})	J_{SC} (mA cm^{-2})	V_{OC} (mV)	*FF*	η (%)
Y123	100	13.9	14.1	867	0.74	9.2
	50	-	7.4	846	0.77	9.4
	10	-	1.4	784	0.79	9.0
WS-70	100	14.1	14.1	903	0.76	9.7
	50	-	7.4	888	0.79	10.0
	10	-	1.4	835	0.80	9.7
WS-72	100	14.2	14.2	926	0.77	10.3
	50	-	7.5	911	0.79	10.5
	10	-	1.5	862	0.80	10.2

J_{SC} (Cal) values were calculated from the IPCE spectra.

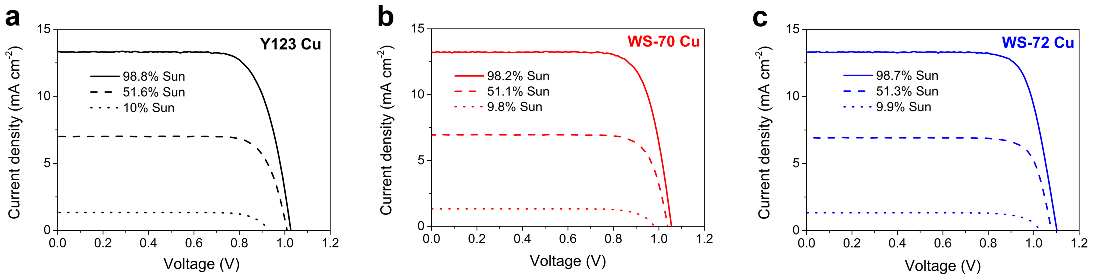

Fig. S3 *J*-*V* curves of the DSSCs fabricated with dye **Y123** (**a**), **WS-70** (**b**) and **WS-72** (**c**) employing $[Cu(tmby)_2]^{2+/+}$ based electrolyte measured under different light intensities (solid, 1 Sun; dashed, 0.5 Sun; dot, 0.1 Sun).

Table S3 Photovoltaic performance of DSSCs fabricated with dyes **Y123**, **WS-70** and **WS-72** with $[Cu(tmby)_2]^{2+/+}$ based electrolyte measured under varied light intensities.

Dye	P_{in} (mW/cm^2)	J_{SC} (Cal) (mA cm^{-2})	J_{SC} (mA cm^{-2})	V_{OC} (V)	*FF*	η (%)
Y123	100	13.6	13.4	1.03	0.74	10.3
	50	-	7.0	1.01	0.78	10.7
	10	-	1.3	0.93	0.79	9.9
WS-70	100	13.5	13.2	1.06	0.77	11.0
	50	-	7.0	1.04	0.79	11.2
	10	-	1.3	0.98	0.79	10.4
WS-72	100	13.3	13.3	1.10	0.78	11.6
	50	-	6.9	1.08	0.80	11.7
	10	-	1.3	1.03	0.78	10.7

J_{SC} (Cal) values were calculated from the IPCE spectra.

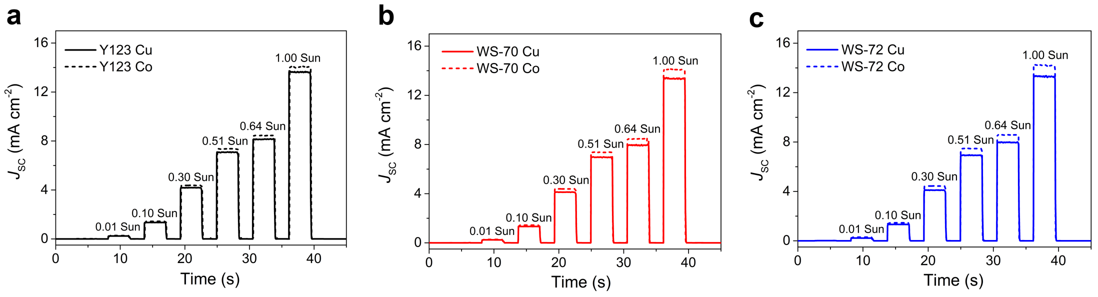

Fig. S4 Dependence of the photocurrent transient dynamics of the DSSCs fabricated with dye **Y123** (**a**), **WS-70** (**b**) and **WS-72** (**c**) measured under different solar light intensities (short dash, $[Co(bpy)_3]^{3+/2+}$ based electrolyte; solid, $[Cu(tmby)_2]^{2+/+}$ based electrolyte).

Table S4 PCE, J_{SC}, V_{OC}, FF, and V_{loss} for some highly performed DSSCs

Dye	References in ESI	PCE (%)	J_{SC} (mA cm^{-2})	V_{OC} (mV)	FF	V_{loss} (mV)
N719	S1	11.2	17.7	846	0.75	720
CYC-B11	S2	11.5	20.1	743	0.77	850
YD2-*o*-C8	S2, S3	11.9	17.3	965	0.71	745
XW11	S4	11.5	20.3	760	0.74	790
Y123	S3	7.1	9.5	986	0.77	890
YA422	S5	10.7	16.3	890	0.74	810
C288	S6	12.0	19.7	843	0.73	710
D35	S7	9.9	12.5	1100	0.72	810
WS-72	This work	11.6	13.3	1100	0.78	600

4. Photophyscical and photokinetic analysis

Table S5 Recombination time constants (τ_{rec}) extracted from flash photolysis measurement.

Dye	**Y123**	**WS-70**	**WS-72**
τ_{rec} (ms)	4.5	9.5	13

Generally, V_{OC} is defined as the energy difference between the quasi-Fermi potential (E^*_{Fn}) in the titania semiconductor and the redox potential (E_{redox}) of the electrolytes. Since the redox potential is identical for a certain cobalt or copper based redox electrolyte, the V_{OC} variation for these dyes can only be attributed to the change of quasi-Fermi potential, which depends on both conduction band edge position and free electron density in TiO_2. As shown in charge extraction measurements (Fig. 5a and 5c), at a given V_{OC}, the extracted charges are almost same for three dyes, suggesting the similar conduction band positions. Then the electron lifetime was measured as a function of V_{OC}, which can provide an insight into the free electron density in TiO_2. As shown in Fig. 5b and 5d, the electron lifetimes are greatly improved from **Y123** to **WS-70** to **WS-72** in both $[Co(bpy)_3]^{3+/2+}$ and $[Cu(tmby)_2]^{2+/+}$ based devices. The long electron lifetime for **WS-72** based devices contributed to the accumulation of electrons in TiO_2 and upwards shifting the E^*_{Fn}, rendering a high V_{OC} performance.

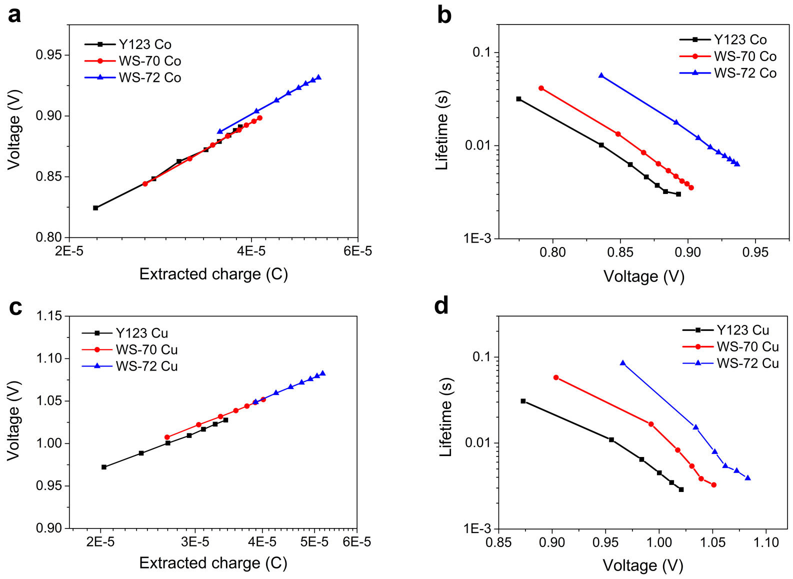

Fig. S5 Charge extraction (**a, c**) and electron lifetime (**b, d**) as a function of V_{OC} for devices fabricated with dye **Y123**, **WS-70** and **WS-72** employing $[Co(bpy)_3]^{3+/2+}$ (**a, b**) and $[Cu(tmby)_2]^{2+/+}$ (**c, d**) based electrolytes.

5. Evolution of photovoltaic performances

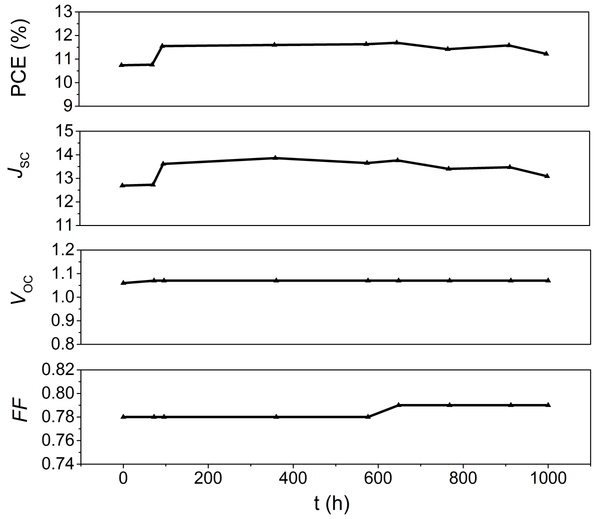

Fig. S6 The shelf lifetime evaluation of the best performing solid state DSSCs fabricated with dye **WS-72** and $[Cu(tmby)_2]^{2+/+}$ based HTM.

6. Element mapping of the dispersion of Cu and Ti elementary in the mesoporous TiO_2 film

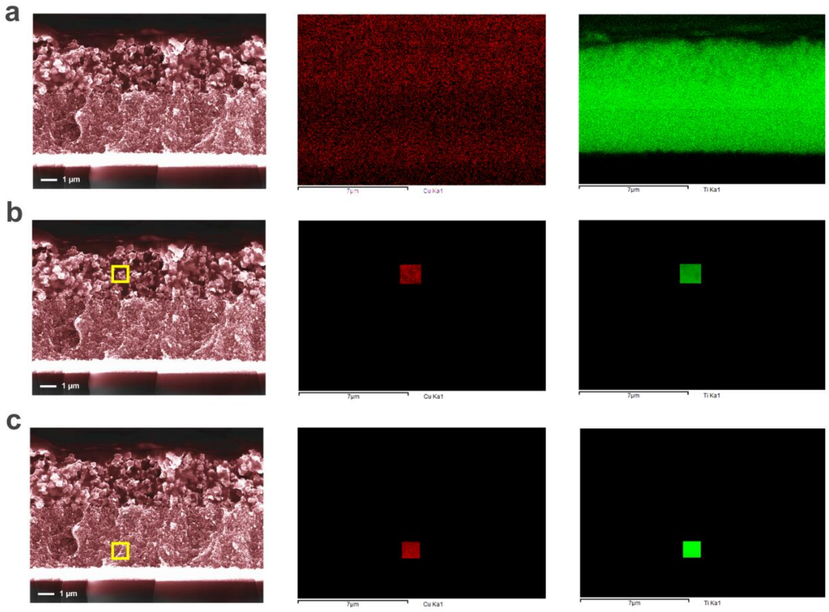

Fig. S7 Cross sectional image (left) of TiO_2 film sensitized by dye **WS-72** infiltrated with $[Cu(tmby)_2]^{2+/+}$ based HTM. Element mapping (right) suggesting the dispersion of Cu (red) and Ti (green) elementary in the mesoporous TiO_2 film (**a**, globle image; **b**, top image; **c**, bottom image).

7. Comparison of electron injection efficiency

Generally, when taking the absorption and reflection of the conductive glass into account, an IPCE plateau of DSSC between 80-90% means internal quantum efficiency is almost unity, which include η_{inj} (electron injection efficiency), η_{reg} (dye regeneration efficiency) and η_{col} (charge collection efficiency). As shown in Fig. 2d, we can see that the dye **WS-72** showed even slightly higher IPCE than dye **WS-70** and **Y123**, although the LUMO energy level of the former is decreased. This means that the modulation of the LUMO energy level here had negligible influence on the electron injection efficiency.

To confirm it, we have carefully compared the light harvesting efficiency (LHE), dye regeneration efficiency (η_{reg}) and charge collection efficiency (η_{col}) by steady state absorption, flash photolysis measurement, and transient photocurrent decay measurement, respectively. The results are shown below. All these measurements did not show any significant difference among the three dyes caused by energy level modulation, further demonstrating the similar electron injection efficiency of three dyes.

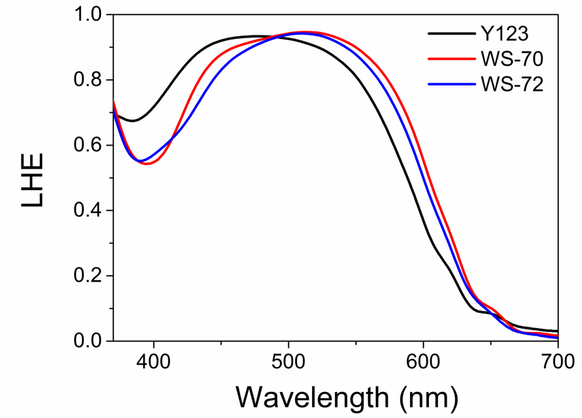

Fig. S8 LHE as a function of wavelength for the dyes **Y123**, **WS-70** and **WS-72** adsorbed on the surface of the 2-μm-thick nanocrystalline TiO_2 film. The LHE for three dyes were very similar on 2-μm-thick TiO_2 film and will further enhance on thicker film in DSSCs devices (4 μm + 4 μm).

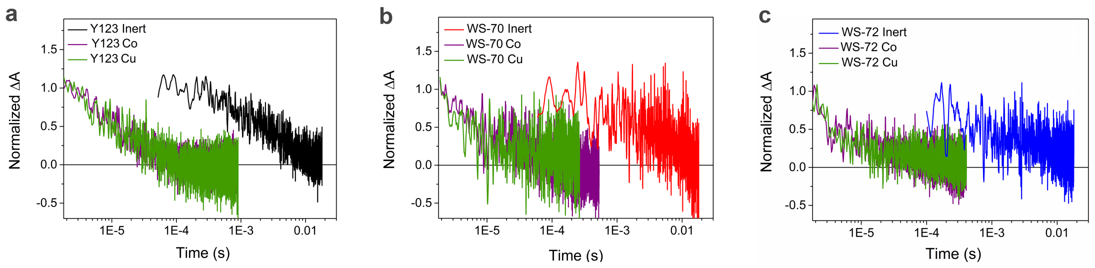

Fig. S9 Flash photolysis measurement of dye **Y123** (a)**, WS-70** (b) and **WS-72** (c) adsorbed on mesoporous TiO_2 films with inert, cobalt (violet) and copper (green) based electrolyte. Excitation wavelength 525 nm, probe wavelength 580 nm for inert electrolyte. Excitation wavelength 525 nm, probe wavelength 500 nm for copper and cobalt based electrolyte.

Table S6 Recombination time constants (τ_{rec}) and regeneration half times ($\tau_{1/2}$) extracted from flash photolysis measurement and calculated dye regeneration yields ($\eta_{reg} = k_{reg} / (k_{reg}+k_{rec})$, $k_i = 1/\tau_i$).

Dye	τ_{rec} (ms)	$\tau_{1/2\ cobalt}$ (μs)	$\eta_{reg\ cobalt}$	$\tau_{1/2\ copper}$ (μs)	$\eta_{reg\ copper}$
Y123	4.5	28	99.4%	26	99.4%
WS-70	9.5	28	99.7%	15	99.8%
WS-72	13	41	99.7%	39	99.7%

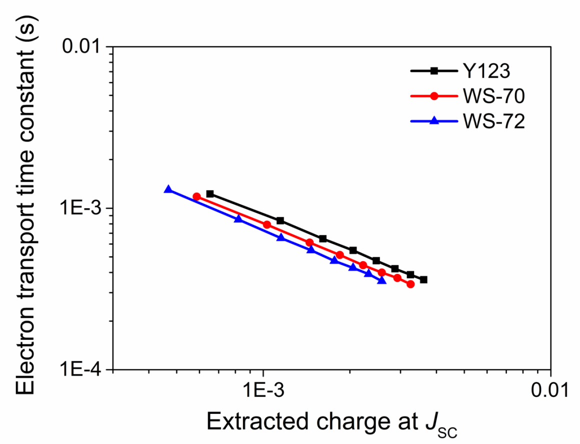

Fig. S10 Electron transport time constant as a function of extracted charge at J_{SC} for DSSCs based on dyes **Y123**, **WS-70** and **WS-72**. The fact that electron transport time constants are similar at a given charge at J_{SC} indicates similar charge collection efficiency.

8. Synthesis and characterizations

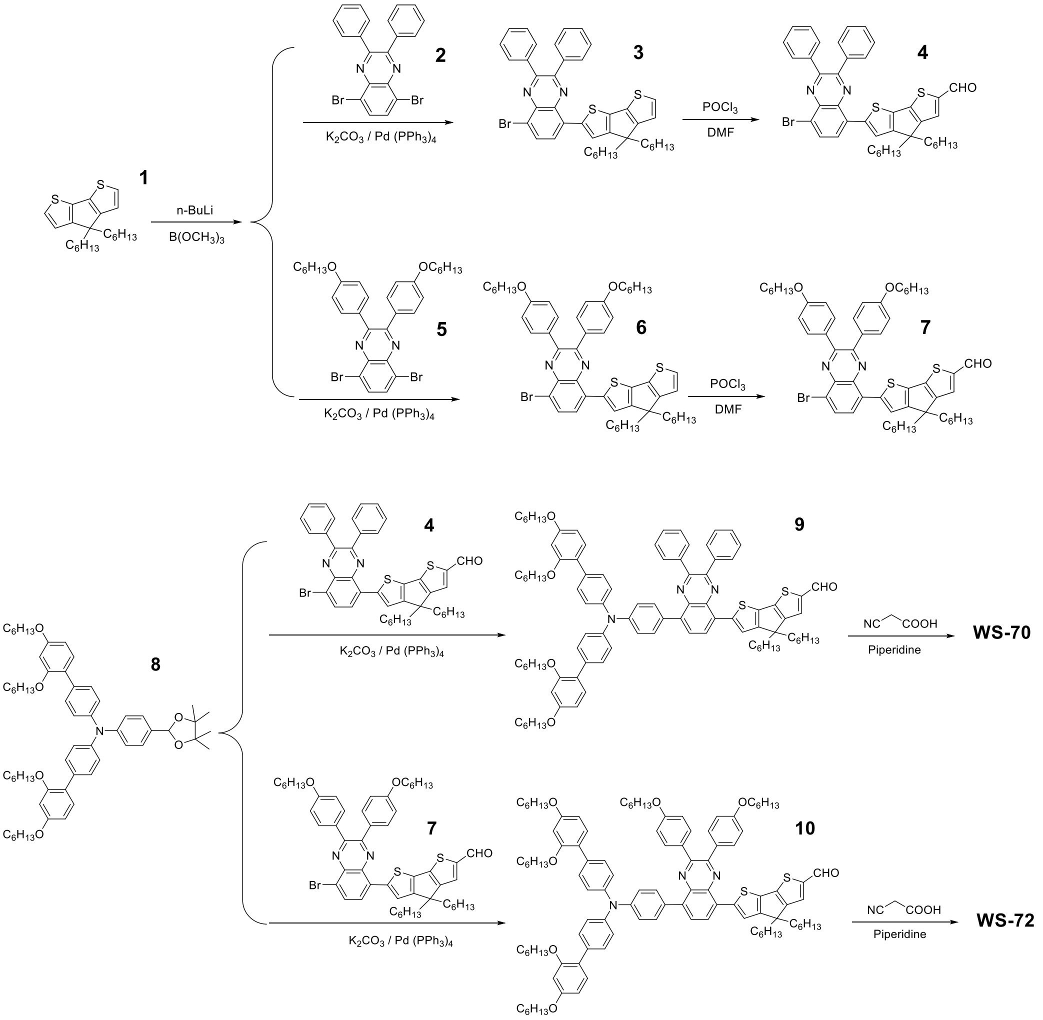

Scheme S1. Synthetic route for dyes **WS-70** and **WS-72**.

Synthesis of compound **3**.

Under argon, to a solution of compound **1** (500 mg, 1.44 mmol) in dry THF (20 mL) was added n-BuLi (0.69 mL, 1.73 mmol) dropwise at -78 °C. The resulting solution was stirred for 1 h before adding $B(OCH_3)_3$ (0.25 mL, 2.20 mmol). The stirring was maintained at -78 °C for another 5 h for next Suzuki reaction without any purification. Under argon, the previous prepared mixture was reacted with compound **2** (707 mg, 1.60 mmol) with 2 M K_2CO_3 (15 mL) and $Pd(PPh_3)_4$ (100 mg) in THF (30 mL) for 8 h. After cooling to the room temperature, the organics solvent were evaporated and the residue was dissolved in CH_2Cl_2 (50 mL) and washed with brine (100 mL) for two times, dried over anhydrous Na_2SO_4, evaporated to remove the solvent. The crude product was then purified by column chromatography on silica gel (Hexane/CH_2Cl_2 = 3/1) to afford a red oil **3** (456 mg, yield 45%).

^{1}H NMR (400 MHz, $CDCl_3$, δ, ppm): 8.06 (d, J = 8.2 Hz, 1 H), 7.99 (d, J = 8.2 Hz, 1 H), 7.81 (s, 1 H), 7.72-7.77 (m, 4 H), 7.38-7.45 (m, 6 H), 7.25 (d, J = 4.8 Hz, 1 H), 6.99 (d, J = 4.8 Hz, 1 H), 1.92 (t, J = 8.3 Hz, 4 H), 1.18-1.24 (m, 12 H), 1.02-1.08 (m, 4 H), 0.81-0.85 (m, 6 H). ^{13}C NMR (100 MHz, $CDCl_3$, δ, ppm): 158.64, 157.76, 153.16, 152.23, 138.87, 138.44, 138.31, 137.85, 133.63, 133.10, 130.48, 130.26, 129.33, 129.23, 128.42, 128.33, 126.26, 125.49, 121.67, 121.64, 121.18, 53.50, 37.94, 31.63, 29.79, 24.62, 22.65, 14.03. HRMS-ESI (*m/z*): [M + H]$^+$ Calcd. for ($C_{41}H_{42}{}^{79}BrN_2S_2$, $C_{41}H_{42}{}^{81}BrN_2S_2$), 705.1973, 707.1959; found: 705.1986, 707.1972.

Synthesis of compound **4**.

Compounds **3** (320 mg, 0.45 mmol) was dissolved in dry DMF (20 mL) at the temperature of 0 °C. $POCl_3$ (1.5 mL, 16.10 mmol) was added dropwise and keep stirring when mixture was gradually warmed to room temperature. CH_3COOK saturated aqueous solution was added to solution to get an alkalescent solution. The mixture was extract with CH_2Cl_2 (50 mL), and washed with brine (200 mL×3), dried over anhydrous Na_2SO_4. The solvent was removed by rotary evaporation, and crude product was purified by column chromatography on silica gel (Hexane/CH_2Cl_2 = 1/1) to give a red powder **4** (296 mg, yield 90%).

^{1}H NMR (400 MHz, $CDCl_3$, δ, ppm): 9.89 (s, 1 H), 8.10 (d, J = 8.2 Hz, 1 H), 8.04 (d, J = 8.2 Hz, 1 H), 7.80 (s, 1 H), 7.74 (t, J = 7.3 Hz, 4 H), 7.62 (s, 1 H), 7.39-7.51 (m, 6 H), 1.91-2.02 (m, 4 H), 1.19-1.25 (m, 12 H), 1.04-1.07 (m, 4 H), 0.82-0.85 (m, 6 H). ^{13}C NMR (100 MHz, $CDCl_3$, δ, ppm): 182.55, 161.72, 158.26, 153.52, 152.70, 148.04, 143.61, 142.91, 139.81, 138.91, 138.23, 138.09, 137.67, 133.07, 132.69, 130.42, 130.26, 129.90, 129.48, 128.43, 128.38, 126.89, 122.81, 121.16, 53.96, 37.85, 31.58, 29.69, 24.68, 22.62, 14.01. HRMS-ESI (*m/z*): [M + H]$^+$ Calcd. for ($C_{42}H_{42}{}^{79}BrN_2OS_2$, $C_{42}H_{42}{}^{81}BrN_2OS_2$), 733.1922, 735.1908; found: 733.1917, 735.1904.

Synthesis of compound **6**.

The compound **6** was synthesized in a similar manner to that for compound **3**.

^{1}H NMR (400 MHz, $CDCl_3$, δ, ppm): 8.00 (d, J = 8.2 Hz, 1 H), 7.93 (d, J = 8.2 Hz, 1 H), 7.70-7.78 (m, 5 H), 7.25 (d, J = 4.8 Hz, 1 H), 7.00 (d, J = 4.8 Hz, 1 H), 6.91-6.98 (m, 4 H), 4.02-4.07 (m, 4 H), 1.91-1.95 (m, 4 H), 1.80-1.89 (m, 4 H), 1.53-1.55 (m, 4 H), 1.39-1.40 (m, 8 H), 1.19-1.25 (m, 12 H), 1.03-1.11 (m, 4 H), 0.94-0.97 (m, 6 H), 0.82-0.85 (m, 6 H). ^{13}C NMR (100 MHz, $CDCl_3$, δ, ppm): 160.31, 160.20, 158.53, 157.73, 152.66, 151.82, 141.06, 138.58, 138.16, 137.44, 137.01, 133.27, 132.52, 131.92, 131.67, 130.89, 130.76, 125.83, 125.35, 121.69, 121.43, 121.11, 114.37, 114.34, 68.12, 53.50, 37.99, 31.68, 31.66, 31.64, 29.85, 29.29, 29.24, 25.79, 25.76, 24.66, 22.69, 22.65, 14.08. HRMS-ESI (*m/z*): [M + H]$^+$ Calcd. for ($C_{53}H_{66}{}^{79}BrN_2O_2S_2$, $C_{53}H_{66}{}^{81}BrN_2O_2S_2$), 905.3749, 907.3740; found: 905.3760, 907.3751.

Synthesis of compound **7**.

The compound **7** was synthesized in a similar manner to that for compound **4**.

^{1}H NMR (400 MHz, $CDCl_3$, δ, ppm): 9.89 (s, 1 H), 8.03 (d, J = 8.1 Hz, 1 H), 7.97 (d, J = 8.2 Hz, 1 H), 7.78 (s, 1 H), 7.72 (t, J = 8.8 Hz, 4 H), 7.63 (s, 1 H), 6.97 (d, J = 8.7 Hz, 2 H), 6.92 (d, J = 8.7 Hz, 2 H), 4.01-4.08 (m, 4 H), 1.93-2.01 (m, 4 H), 1.80-1.90 (m, 4 H), 1.49-1.55 (m, 4 H), 1.38-1.41 (m, 8 H), 1.19-1.25 (m, 12 H), 1.05-1.08 (m, 4 H), 0.94-0.98 (m, 6 H), 0.82-0.86 (m, 6 H). ^{13}C NMR (100 MHz, $CDCl_3$, δ, ppm): 182.53, 161.70, 160.42, 160.39, 158.18, 153.01, 152.28, 148.19, 143.49, 143.22, 139.67, 138.60, 137.36, 132.47, 132.31, 131.88, 131.67, 130.65, 130.47, 129.94, 126.38, 122.66, 120.86, 114.40, 68.18, 68.13, 53.94, 37.86, 31.63, 31.61, 29.72, 29.26, 29.21, 25.76, 25.74, 24.69, 22.63, 14.06, 14.02. HRMS-ESI (*m/z*): [M + H]$^+$ Calcd. for ($C_{54}H_{66}{}^{79}BrN_2O_3S_2$, $C_{54}H_{66}{}^{81}BrN_2O_3S_2$), 933.3698, 935.3689; found:

933.3690, 935.3683.

Synthesis of compound **9**.

The compound **8** (170 mg, 0.18 mmol), **4** (100 mg, 0.14 mmol) were mixed with 2 M K_2CO_3 (15 mL) and $Pd(PPh_3)_4$ (100 mg) in THF (30 mL), the reaction mixture was heated to 80 °C and stirred for 8 h. After completion of the reaction, the organics were evaporated and the residue was dissolved in CH_2Cl_2 (50 mL) and washed with brine (100 mL×3), dried over anhydrous Na_2SO_4, evaporated to remove the solvent. The crude product was then purified by column chromatography on silica gel (Hexane/CH_2Cl_2 = 1/1) to afford a red oil **9** (138 mg, 68%).

^{1}H NMR (400 MHz, $CDCl_3$, δ, ppm): 9.89 (s, 1 H), 8.27 (d, J = 8.0 Hz, 1 H), 7.94 (d, J = 7.9 Hz, 1 H), 7.80-7.86 (m, 5 H), 7.65-7.67 (m, 2 H), 7.63 (s, 1 H), 7.52-7.54 (m, 4 H), 7.46-7.48 (m, 3 H), 7.29-7.38 (m, 11 H), 6.59-6.60 (m, 4 H), 4.00-4.05 (m, 8 H), 1.97-2.01 (m, 4 H), 1.77-1.88 (m, 8 H), 1.50-1.54 (m, 4 H), 1.45-1.48 (m, 4 H), 1.38-1.41 (m, 8 H), 1.33-1.35 (m, 8 H), 1.21-1.24 (m, 12 H), 1.08-1.09 (m, 4 H), 0.94-0.97 (m, 6 H), 0.88-0.92 (m, 6 H), 0.83-0.87 (m, 6 H). ^{13}C NMR (100 MHz, $CDCl_3$, δ, ppm): 182.48, 161.85, 159.60, 158.05, 157.02, 151.80, 151.38, 148.54, 147.79, 145.74, 144.17, 143.24, 139.22, 138.86, 138.81, 138.74, 138.70, 137.12, 133.31, 131.61, 131.17, 130.89, 130.44, 130.25, 130.16, 129.91, 129.32, 129.18, 129.00, 128.38, 128.25, 126.89, 124.21, 123.05, 122.48, 120.58, 105.38, 100.49, 68.46, 68.15, 53.90, 37.93, 31.64, 31.61, 31.47, 29.73, 29.35, 29.10, 25.79, 25.78, 24.69, 22.64, 22.59, 14.07, 14.05, 14.03. HRMS-ESI (*m/z*): $[M + H]^+$ Calcd. for ($C_{96}H_{111}N_3O_5S_2$), 1450.8043; found: 1450.7941.

Synthesis of compound **WS-70**.

Under argon, compound **5** (116 mg, 0.08 mmol) and cyanoacetic acid (100 mg, 1.18 mmol) were dissolved in chloroform (20 mL) with piperidine (0.50 mL). The mixture was heated to 72°C and refluxed for 8 h. Then the solvent was removed under reduced pressure. The residue was dissolved in CH_2Cl_2 (50 mL) and washed with brine (100 mL×3), dried over anhydrous Na_2SO_4, evaporated to remove the solvent and purified by column chromatography on silica gel (CH_2Cl_2/MeOH = 10/1) to afford a dark solid **WS-70** (79 mg, 65%).

^{1}H NMR (400 MHz, Acetone-d$_6$, δ, ppm): 8.50 (d, J = 5.7 Hz, 1 H), 8.46 (s, 1 H), 8.22 (s, 1 H), 7.98-8.03 (m, 2 H), 7.91 (d, J = 7.4 Hz, 2 H), 7.82 (d, J = 7.0 Hz, 2 H), 7.69 (d, J = 7.2 Hz, 2 H), 7.53 (d, J = 8.0 Hz, 4 H), 7.48-7.49 (m, 3 H), 7.36-7.40 (m, 3 H), 7.21-7.30 (m, 8 H), 6.66 (s, 2 H), 6.61 (d, J = 8.4 Hz, 2 H), 4.03-4.06 (m, 8 H), 1.73-1.84 (m, 10 H), 1.45-1.52 (m, 10 H), 1.37-1.39 (m, 8 H), 1.31 (m, 8 H), 1.19-1.21 (m, 12 H), 1.10 (m, 4 H), 0.92-0.95 (m, 6 H), 0.84-0.88 (m, 6 H), 0.79-0.82 (m, 6 H). ^{13}C NMR (100 MHz, Acetone-d$_6$, δ, ppm): 163.67, 162.59, 159.89, 158.62, 157.09, 152.11, 151.58, 149.44, 147.68, 147.09, 145.62, 144.77, 139.44, 139.12, 138.77, 138.61, 136.86, 136.60, 133.86, 131.80, 131.54, 131.12, 130.66, 130.42, 130.31, 130.09, 129.45, 129.10, 128.89, 128.28, 128.09, 127.17, 124.01, 122.60, 122.03, 121.22, 116.84, 105.84, 100.25, 70.33, 68.14, 67.76, 53.88, 37.58, 31.47, 31.33, 25.67, 25.63, 24.47, 22.42, 22.40, 22.34, 13.46, 13.43, 13.37. HRMS-ESI (*m/z*): $[M + H]^+$ Calcd. for ($C_{99}H_{113}N_4O_6S_2$), 1517.8102; found: 1517.8054.

Synthesis of compound **10**.

The compound **10** was synthesized in a similar manner to that for compound **9**.
^{1}H NMR (400 MHz, $CDCl_3$, δ, ppm): 9.90 (s, 1 H), 8.22 (d, J = 8.0 Hz, 1 H), 7.89 (d, J = 7.9 Hz, 1 H), 7.79-7.86 (m, 5 H), 7.64-7.66 (m, 3 H), 7.53-7.55 (m, 4 H), 7.29-7.30 (m, 8 H), 6.99 (d, J = 8.7 Hz, 2 H), 6.88 (d, J = 8.7 Hz, 2 H), 6.59-6.61 (m, 4 H), 3.99-4.10 (m, 12 H), 1.98-2.02 (m, 4 H), 1.78-1.90 (m, 12 H), 1.51-1.55 (m, 8 H), 1.43-1.49 (m, 6 H), 1.34-1.43 (m, 24 H), 1.22-1.25 (m, 12 H), 1.09 (m, 4 H), 0.95-0.98 (m, 10 H), 0.89-0.93 (m, 6 H), 0.84-0.88 (m, 6 H). ^{13}C NMR (100 MHz, $CDCl_3$, δ, ppm): 182.47, 161.85, 160.16, 160.00, 159.60, 158.00, 157.03, 151.33, 150.96, 148.68, 147.67, 145.80, 144.45, 143.14, 139.13, 138.57, 138.45, 136.86, 133.24, 131.83, 131.62, 131.50, 131.29, 131.09, 130.88, 130.24, 129.96, 128.97, 128.81, 128.54, 128.42, 126.40, 124.15, 123.07, 122.59, 120.32, 114.38, 114.29, 105.39, 100.50, 68.47, 68.15, 68.08, 53.90, 37.95, 31.65, 31.63, 31.48, 29.76, 29.36, 29.30, 29.24, 29.12, 25.81, 25.79, 25.74, 24.71, 22.66, 14.06. HRMS-ESI (*m/z*): $[M + H]^+$ Calcd. for ($C_{108}H_{135}N_3O_7S_2$), 1650.9820; found: 1650.9778.

Synthesis of compound **WS-72**.
The compound **WS-72** was synthesized in a similar manner to that for compound **WS-70**.
^{1}H NMR (400 MHz, $CDCl_3$, δ, ppm): 8.40 (s, 1 H), 8.22 (d, J = 7.8 Hz, 1 H), 7.77-7.88 (m, 6 H), 7.69 (s, 1 H), 7.63 (d, J = 8.5 Hz, 2 H), 7.52 (d, J = 8.4 Hz, 4 H), 7.29-7.41 (m, 8 H), 7.02 (d, J = 8.6 Hz, 2 H), 6.87 (d, J = 8.6 Hz, 2 H), 6.58-6.60 (m, 4 H), 3.97-4.11 (m, 12 H), 2.00 (m, 4 H), 1.77-1.88 (m, 12 H), 1.50-1.54 (m, 8 H), 1.44-1.48 (m, 6 H), 1.33-1.41 (m, 24 H), 1.21 (m, 12 H), 1.07 (m, 4 H), 0.94-0.97 (m, 10 H), 0.88-0.91 (m, 6 H), 0.83-0.86 (m, 6 H). ^{13}C NMR (100 MHz, $CDCl_3$, δ, ppm): 163.12, 160.21, 159.99, 159.59, 158.95, 157.02, 151.44, 151.18, 147.73, 145.77, 139.24, 138.96, 138.40, 136.86, 136.21, 133.25, 131.71, 131.64, 131.50, 131.37, 131.28, 130.95, 130.88, 130.62, 130.24, 128.72, 128.60, 127.02, 126.70, 124.16, 123.07, 122.53, 120.24, 114.54, 114.28, 105.38, 100.49, 68.46, 68.15, 53.86, 38.00, 31.65, 31.64, 31.61, 31.60, 31.47, 29.35, 29.10, 25.79, 25.77, 22.64, 22.61, 22.59, 14.06, 14.05, 14.03. HRMS-ESI (*m/z*): $[M + H]^+$ Calcd. for ($C_{111}H_{137}N_4O_8S_2$), 1717.9878; found: 1717.9808.

^{1}H, ^{13}C NMR of intermediates and targeted sensitizers.

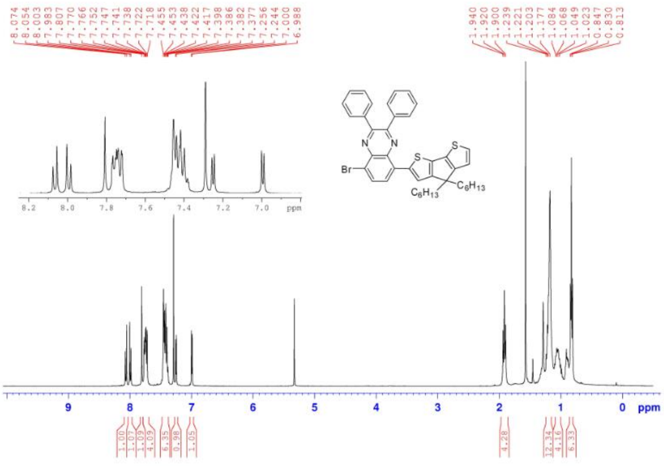

Fig. S11 ^{1}H NMR of compound **3** recorded in $CDCl_3$.

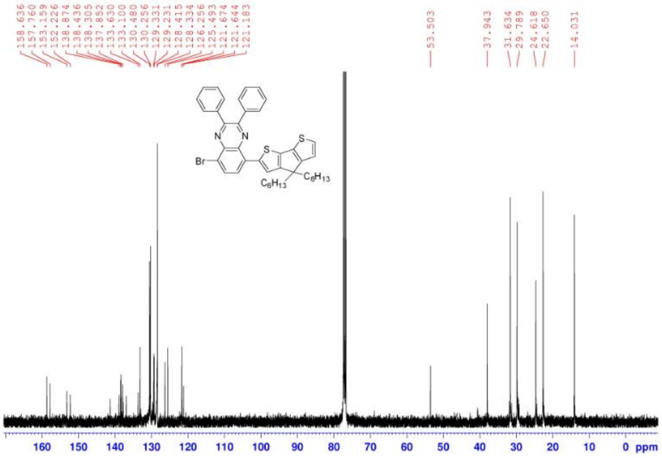

Fig. S12 ^{13}C NMR of compound **3** recorded in $CDCl_3$.

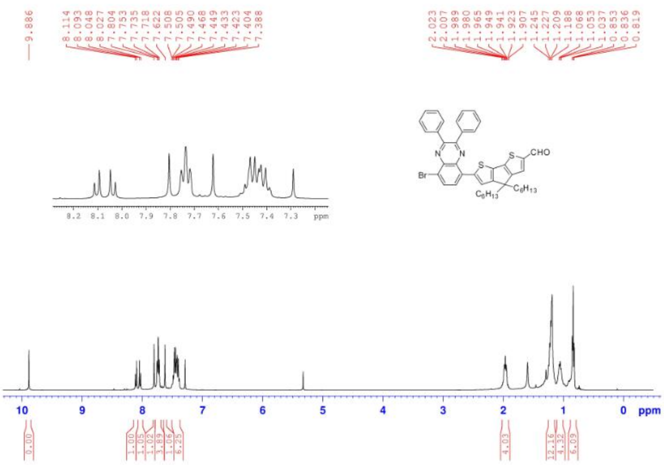

Fig. S13 ^{1}H NMR of compound **4** recorded in $CDCl_3$.

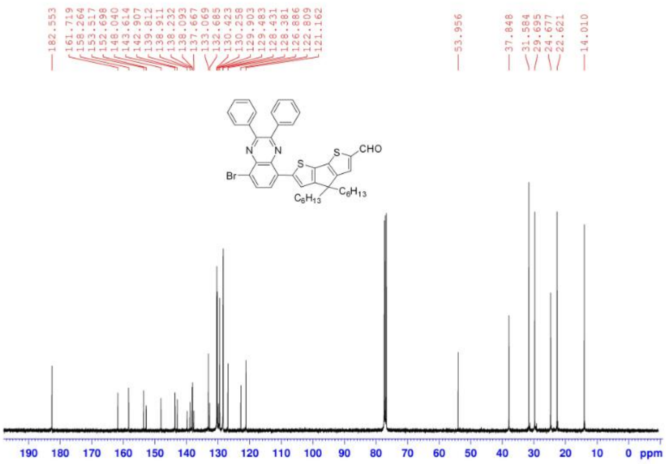

Fig. S14 ^{1}H NMR of compound **4** recorded in $CDCl_3$.

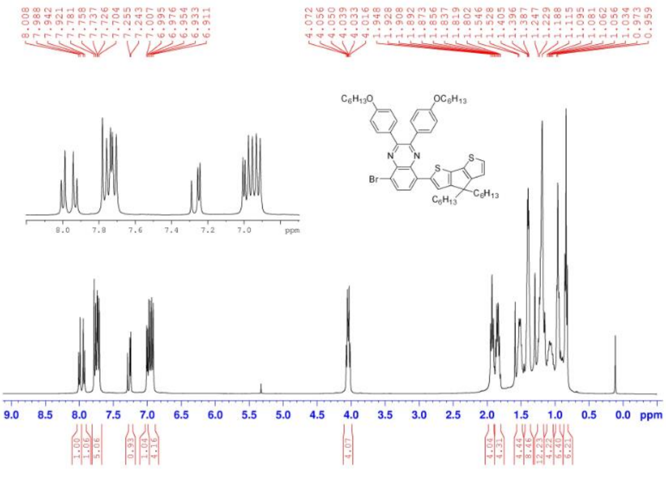

Fig. S15 ^{1}H NMR of compound **6** recorded in $CDCl_3$.

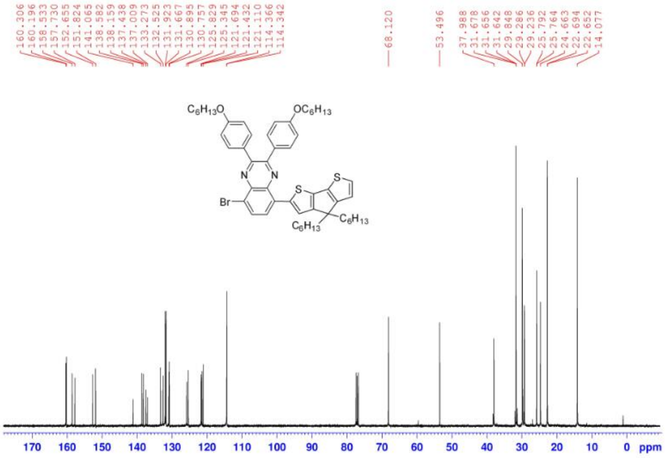

Fig. S16 ^{1}H NMR of compound **6** recorded in $CDCl_3$.

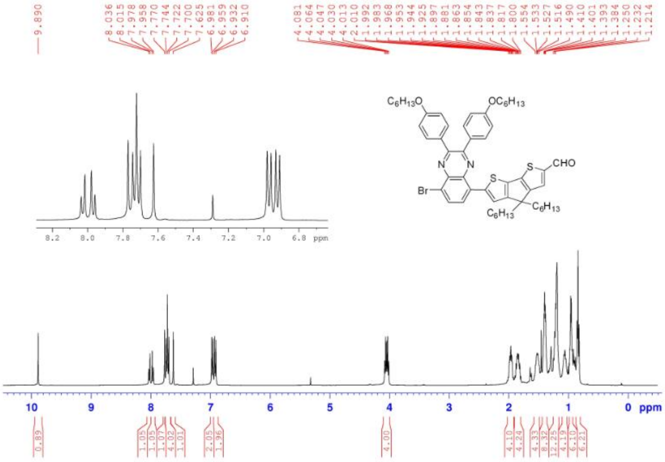

Fig. S17 ^{1}H NMR of compound **7** recorded in $CDCl_3$.

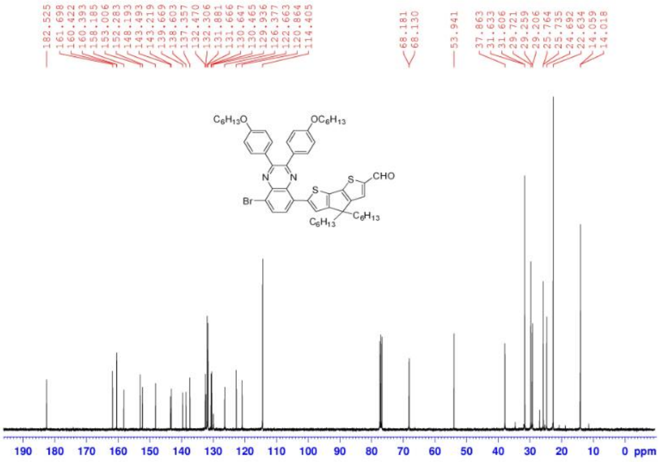

Fig. S18 ^{13}C NMR of compound **7** recorded in $CDCl_3$.

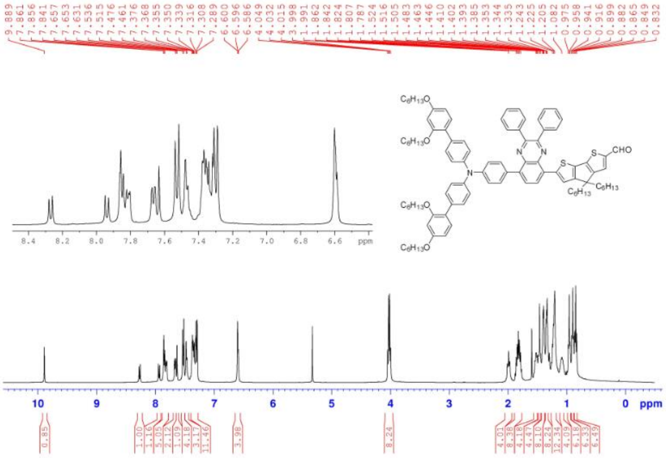

Fig. S19 ^{1}H NMR of compound **9** recorded in $CDCl_3$.

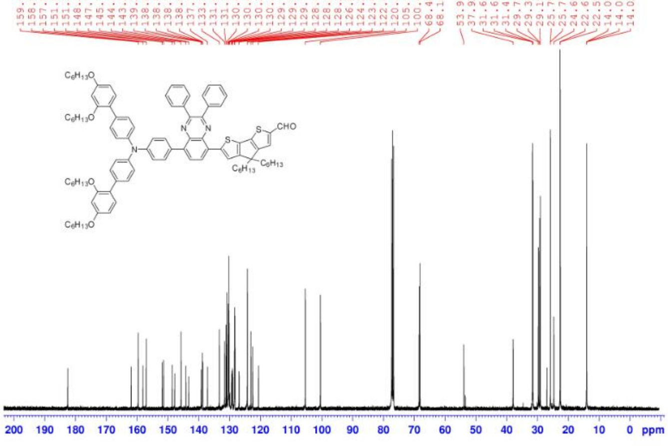

Fig. S20 ^{13}C NMR of compound **9** recorded in $CDCl_3$.

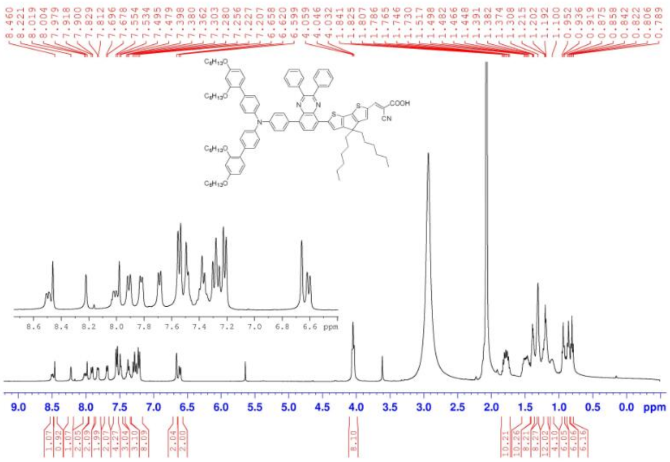

Fig. S21 ^{1}H NMR of compound **WS-70** recorded in Acetone-d$_6$.

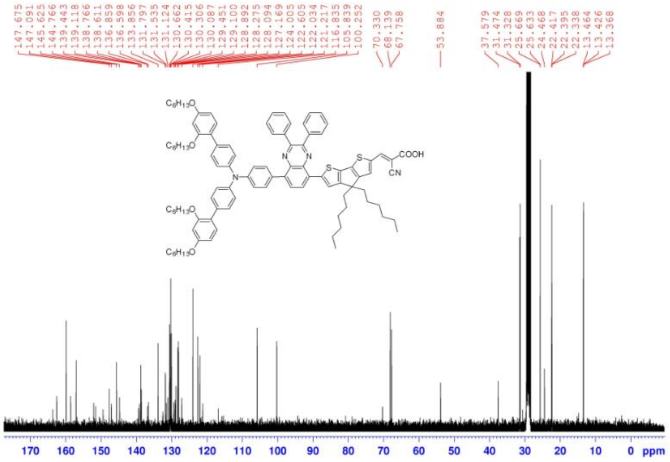

Fig. S22 ^{13}C NMR of compound **WS-70** recorded in Acetone-d$_6$.

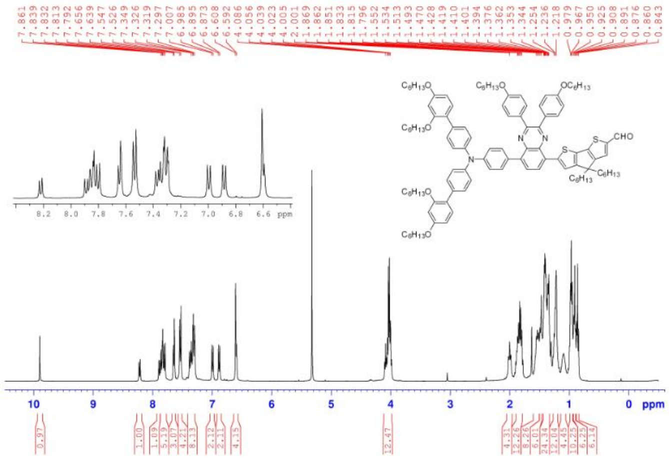

Fig. S23 ^{1}H NMR of compound **10** recorded in $CDCl_3$.

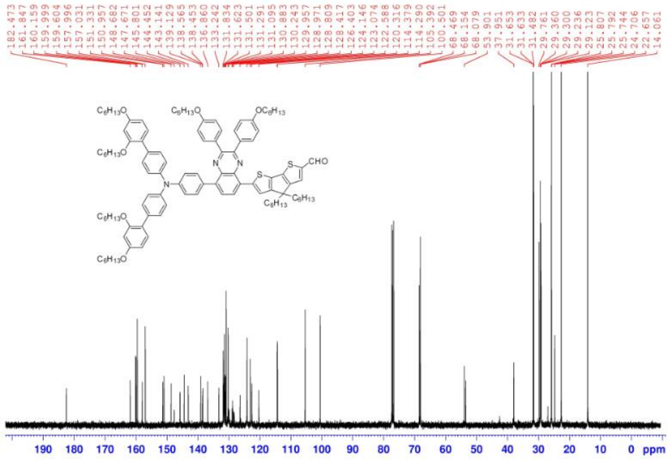

Fig. S24 ^{13}C NMR of compound **10** recorded in $CDCl_3$.

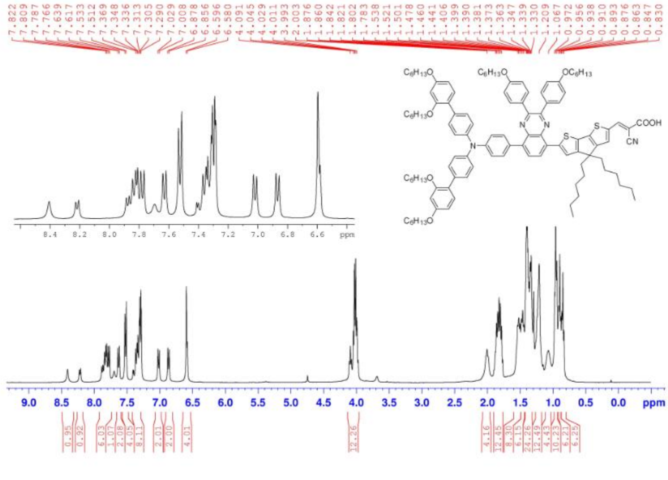

Fig. S25 ^{1}H NMR of compound **WS-72** recorded in $CDCl_3$.

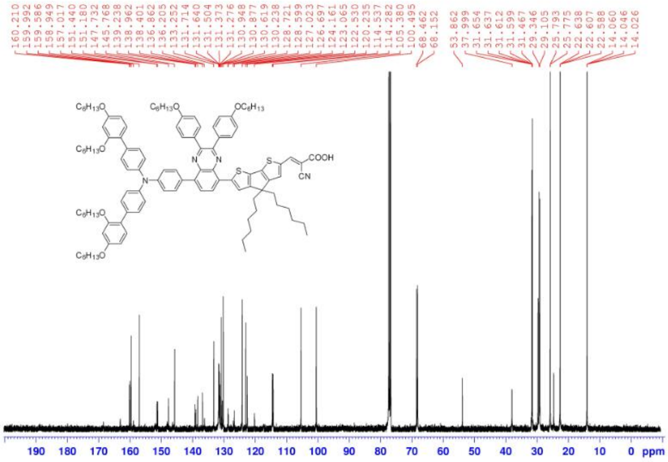

Fig. S26 ^{13}C NMR of compound **WS-72** recorded in $CDCl_3$.

Supplementary References

S1 M. K. Nazeeruddin, F. De Angelis, S. Fantacci, A. Selloni, G. Viscardi, P. Liska, S. Ito, B. Takeru and M. Grätzel, *J. Am. Chem. Soc.*, 2005, **127**, 16835-16847.

S2 B. E. Hardin, H. J. Snaith, M. D. McGehee, *Nat. Photonics*, 2012, **6**, 162-169.

S3 A. Yella, H. W. Lee, H. N. Tsao, C. Yi, A. K. Chandiran, M. K. Nazeeruddin, E. W. G. Diau, C. Y. Yeh, S. M. Zakeeruddin, M. Grätzel, *Science*, 2011, **334**, 629-634.

S4 Y. Xie, Y. Tang, W. Wu, Y. Wang, J. Liu, X. Li, H. Tian and W. Zhu, *J. Am. Chem. Soc.*, 2015, **137**, 14055-14058.

S5 J. Yang, P. Ganesan, J. Teuscher, T. Moehl, Y. J. Kim, C. Yi, P. Comte, K. Pei, T. W. Holcombe, M. K. Nazeeruddin, J. Hua, S. M. Zakeeruddin, H. Tian and M. Grätzel, *J. Am. Chem. Soc.*, 2014, **136**, 5722-5730.

S6 Y. Ren, Y. Li, S. Chen, J. Liu, J. Zhang and P. Wang, *Energy Environ. Sci.*, 2016, **9**, 1390-1399.

S7 M. Freitag, J. Teuscher, Y. Saygili, X. Zhang, F. Giordano, P. Liska, J. Hua, S. M. Zakeeruddin, J. Moser, M. Grätzel, A. Hagfeldt, *Nat. Photonics*, 2017, **11**, 372-378.